OPEN ACCESS Freely available online

AFM Applied Functional Materials

ISSN 2737-5323
Volume 1, Issue 1
https://www.iikii.com.sg/journal/AFM
Applied Functional Materials

Article

Ultraviolet Light Exposure Effect on the Nanoscale Current-Voltage Characteristics of Bare and Silicate Nanoparticle Incorporated 3-aminopropyltrimethylsiloxane Films Deposited Using a Focus Ion Beam-Milled Atomic Force Microscopy Tip

Su-Yu Liao [1], Jheng-Jia Jhuang [1], Jing-Jenn Lin [2], Congo Tak-Shing Ching [3,*], and You-Lin Wu[1],**

[1] Department of Electrical Engineering, National Chi Nan University, Puli, Nantou, 545, Taiwan. R.O.C.; suyu@ncnu.edu.tw ; s105323904@mail1.ncnu.edu.tw; ylwu@ncnu.edu.tw
[2] Department of Applied Materials and Optoelectronic Engineering, National Chi Nan University, Puli, Nantou, 545, Taiwan, R.O.C.; cclin@ncnu.edu.tw
[3] Graduate Institute of Biomedical Engineering, National Chung Hsing University, Taichung, 402, Taiwan. R.O.C. ; tsching@nchu.edu.tw
Correspondence : **: ylwu@ncnu.edu.tw (Y-L.W); *tsching@nchu.edu.tw (C.T-S. C)

Received: Jun 14, 2021; **Accepted:** Jul 20, 2021; **Published:** Aug 30, 2021

Abstract: Polysilicon wire (PSW) sensor with a sensing membrane of 3-aminopropyltrimethylsiloxan (γ-APTES) incorporated with polydimethylsiloxane (PDMS)-treated silica nanoparticles (NPs) (γ-APTES+NPs nanocomposite) deposited by a focus ion beam (FIB)-milled capillary atomic force microscopy (AFM) tip have been reported to have excellent biochemical sensing characteristics, and improved performance can be achieved after the sensing films being subjected to ultraviolet (UV) light illumination. While most of the research on γ-APTES is focused on its sensing characteristics and material properties, rarely have been discussed regarding its electrical characteristics. In this work, nanoscale current-voltage (I-V) characteristics of the FIB-milled capillary AFM tip deposited pure γ-APTES film and γ-APTES+NPs nanocomposite films with different γ-APTES/NPs mixed ratios were measured by using an AFM with a conductive tip as the top electrode. The I-V characteristics of the γ-APTES and γ-APTES+NPs films after UV illumination were also investigated. Our experimental results show that the nanoscale I-V curve of the γ-APTES-based films is similar to that of a typical dielectric film, and the nanoscale bulk leakage current decreases with the increase of the UV exposure time and the γ-APTES solution/NPs mixed ratios, while the breakdown voltage increases with increasing UV exposure time but decreases with the increase of γ-APTES solution/NPs mixed ratios.

Keywords: 3-aminopropyltrimethylsiloxane; atomic force microscopy; biochemical sensor; sensing membrane; silicate nanoparticles; UV curing.

1. Introduction

The sensing membrane constitutes the most critical part in biochemical sensors because it is utilized to catch the targeted biological species and transform it into a measurable signal. Among the various sensing materials, γ-APTES is commonly used for biochemical sensors. The large amount of amino groups ($CH\text{-}NH_2$) on its surface makes it bond easily with hydrogen ions or hydrogen ion-related biomolecules. Biochemical sensors using γ-APTES as a sensing membrane have been reported for pH [1], glucose [2–4], DNA [5-7], and cell [8, 9] sensing. In addition, substantial extant literature demonstrated that adding nanoparticles to the sensing membrane can augment the sensitivity of sensors because the surface-to-volume ratio of the sensing film is increased [10-15]. Indeed, our previous research has also shown that, through using γ-APTES plus PDMS-treated silica NPs (γ-APTES+NPs) as a sensing membrane, PSW can be employed for biochemical detection efficiently with excellent sensitivity, improved lowest detection limit, and good interference immunity [2,4,6,8]. However, a key factor to achieve those detections with PSW is the requirement of a FIB-milled capillary AFM tip, at which there is a small cylindrical well dug by the FIB milling process. Details on the fabrication of the FIB-milled capillary AFM tip can be found elsewhere [2]. The small well has a dimension of 2.5 μm in diameter and a depth of 4 μm, such that it can carry a tiny amount of sensing membrane nanocomposite material, as well as targeted species solutions, for measurement by capillary effect to the sensing location (gate area) and dropping them onto the PSW. On the other hand, most existing analyses on γ-APTES and γ-APTES+NPs sensing membranes have been

carried out by Fourier Transform Infrared Spectroscopy (FTIR) [16-20]. Electrical characterization on the γ-APTES and γ-APTES+NPs films themselves, as well as electrical characterization on the γ-APTES and γ-APTES+NPs films deposited by the FIB-milled capillary AFM tip are barely found in the literature. Since the amount of solution that the well can carry is estimated to be $\sim 3\times10^{-2}$ pL from the volume of the cylindrical well, the area of the films deposited by using the FIB-milled capillary AFM tip is quite small, and it is challenging to perform conventional electrical characterization on the film itself. Therefore, in this work, we deposited the γ-APTES and γ-APTES+NPs films by the FIB-milled capillary AFM tip, and measured their nanoscale I-V characteristics by using a conductive AFM tip. It is worth noting that, with the assistance of surface morphology scan by AFM, the conductive AFM tip can be placed to any pre-defined position on the sample surface. Moreover, our previous preliminary research has demonstrated that the γ-APTES+NPs film structure can be enhanced after UV light exposure [18], and therefore the effect of post-deposition UV light exposure on the electrical characteristics of the γ-APTES and γ-APTES+NPs films deposited by FIB-milled capillary AFM tip is investigated in this work.

2. Materials and Methods

A p-type (100) silicon (Si) wafer was back-contacted with a 100 nm-thick aluminum (Al) layer after a standard semiconductor clean process. The Si wafer used has a sheet resistance of 40 - 50 Ω/Square. The surface native oxide of the Si wafer was striped by buffer HF solution in the final step of the wafer clean process, such that there is no contact resistance between the sample and the Al layer. First, we mixed pure γ-APTES powder with ethanol solution to form γ-APTES solution with a fixed volume ratio of 1:100, and then PDMS-treated hydrophobic fumed silica NPs (R202, EVONIC industries) was added to the γ-APTES solution with various γ-APTES solution/NPs weight ratios (100:1, 145:1, 200:1, 500:1, and 1000:1, respectively). The average primary silica particle size was approximately 14 nm in diameter. Each of the final γ-APTES+NPs nanocomposite solutions was then subjected to ultrasonic vibration for 10 min to disperse the silica NPs. A micropipette was used to load either the solution of γ-APTES or γ-APTES + NPs mixture into the cylindrical well of the FIB-milled capillary tip. The capillary AFM tip was then placed onto the Si wafer surface with a contact force of 1 nN, and an area of 3 μm × 3 μm was scanned so that the mixture in the cylindrical well was coated over the scanned area simultaneously. All of the coated samples were then cured on a hotplate at 120 °C for 5 min, followed by UV light (λ= 365 nm) exposure with a time range from 0 to 120 s. After preparation of the samples, AFM with a conventional PtIr conductive tip was utilized to perform the topographic scan, and measure the surface morphologies of each coated sample under tapping mode with a resonant frequency of 14 kHz, a force constant of 0.2 N/m, and a speed of 1 Hz. Figure 1 schematically shows the coating of γ-APTES+NPs solution onto the silicon surface by using the FIB-milled capillary AFM tip. The inset shown in Fig. 1 is the scanning electron microscopy (SEM) image of the FIB-milled capillary AFM tip, in which the small well is clearly observed. Since the maximum current that the source measurement unit (SMU) of the AFM can be measured is limited to below 100 pA, it is necessary to extend the current measurement capability of the AFM. To achieve this, we connected the semiconductor parameter analyzer Agilent 4156C to our AFM system, and details of which can be found in reference [21]. A conductive PtIr AFM tip with an tip radius of less than 24 nm was used to measure the nanoscale bulk leakage current of the γ-APTES and γ-APTES+NPs films as a function of the applied voltage under contact mode. The average contact area between the AFM tip and the sample surface is around 1.8×10^{-11} cm^2. Figure 2 schematically illustrates the structure of the sample measurement as well as the measurement setup in this work. Apparently, the overall measurement structure is similar to a miniaturized metal-insulator-semiconductor capacitor with the AFM conductive tip as the top electrode, and the γ-APTES-based film plus the native oxide as the insulator. As a consequence, the measured current in this work can be viewed as the bulk leakage current of the γ-APTES-based films.

3. Results

Since the coated film area is quite small, surface morphology scans of the deposited films were carried out first to determine the precise positions onto which the highly localized nanoscale electrical field was applied. Figure 3 depicts the typical AFM images of the γ-APTES+NPs membrane (with a fixed γ-APTES solution/NPs weight ratio of 100:1) after being subjected to UV light illumination for times ranging from 0 to 120 s. As observed, the film surface is rough and replete with bumpy bead-like particles due to the incorporation of silica NPs in the γ-APTES films. By careful inspection of the images, we can find that the bumpy characteristic of the surface becomes clearer with increasing UV light exposure time, indicating that those NPs seem to be more tightly bound to the γ-APTES. This suggests that the UV light illumination could strengthen the binding between the γ-APTES molecules and silica NPs. This is in accordance with the FTIR analysis results given in reference [18]. With the assistance of the scanned AFM images shown in Fig. 3, it is possible to place the conductive AFM tip at any pre-selected location on the γ-APTES or γ-APTES+NPs film surface and measure the nanoscale I-V characteristics. It should be noticed that the nanoscale bulk leakage current is different when placing the conductive AFM tip at the convex and concave locations on the surface of the γ-APTES+NPs films because of the film thickness difference. In general, the nanoscale leakage current is higher and the breakdown voltage lower at the convex location than at the concave position of the γ-APTES and γ-APTES+NPs films prepared under the same condition. In order to make fair comparisons, all the subsequent I-V characteristics were taken at the convex position on the surface of the deposited films. Figure 4 shows the nanoscale I-V characteristics of the γ-APTES and γ-APTES+NPs films after being exposed to UV light with various exposure times. The mixture ratio of γ-APTES solution/NPs here is fixed to 100:1. Apparently, the leakage current flowing through γ-APTES film is roughly four orders of magnitude higher than the one through γ-APTES+NPs. The loose molecular structure and low resistivity nature of the γ-APTES film explains why the current is much higher, and no breakdown occurs up to an AFM tip voltage of 8 V. The I-V characteristics shown in Fig. 4 also imply that the incorporation of PDMS-treated silica NPs alters the chemical bonding in the γ-APTES films. The strong binding between the NPs and the γ-APTES molecules give rise to a marked change in the γ-APTES structure and strengthen the bulk structure of the films. Furthermore, a sudden leakage current increase, similar to a dielectric breakdown, is observed for the γ-APTES+NPs membranes, which is to the I-V characteristics of common dielectrics [22]. As observed, both the leakage current flowing through the γ-APTES+NPs and the breakdown voltage are different for various UV exposure time. To further confirm the effect of UV light exposure on the sensing membrane, we extracted the leakage current at an AFM tip voltage of 3 V and the breakdown voltage from the I-V characteristics as a function of UV light exposure time, and plotted them in Fig. 5(a) and 5(b), respectively. As observed, the nanoscale bulk leakage current decreases, while the breakdown voltage increases, with the increase of the UV light exposure time. Clearly, the membrane with a γ-APTES solution/silica NPs mixed ratio of 100:1 plus a treatment of 120 s UV yields the highest breakdown voltage, as well as the lowest bulk leakage current. This again indicates that UV light exposure can assist to strengthen the coated γ-APTES+NPs membrane structure.

The effects of the γ-APTES solution/NPs mixed ratio on the nanoscale bulk leakage current of the sensing membrane were also investigated in this work by fixing the UV exposure time to 120 s. Figure 6 shows the nanoscale I-V characteristics of the γ-APTES+NPs films with various γ-APTES solution/NPs mixed ratios plus 120 s UV light exposure using the conductive AFM tip as the top electrode. Apparently, both the nanoscale bulk leakage current and the breakdown voltage of the γ-APTES+NPs films are different for various γ-APTES solution/NPs mixed ratios. The corresponding breakdown voltages are 5.8 V, 5.3 V, 5.1 V, 4.8 V, and 4.4 V for the γ-APTES+NPs membranes with mixed ratios of 100:1, 145:1, 200:1, 500:1, and 1000:1, respectively. In order to obtain additional insight into the effect of mixed ratios of the γ-APTES+NPs membrane on the bulk leakage current, we extracted the leakage currents at an AFM tip voltage of 2.7 V and the breakdown voltages from the I-V characteristics as a function of γ-APTES solution/NPs mixed ratio, and plotted them in Fig. 7(a) and 7(b), respectively. As observed, the nanoscale bulk leakage current increases, while the breakdown voltage decreases, with increasing γ-APTES solution/NPs mixed ratio.

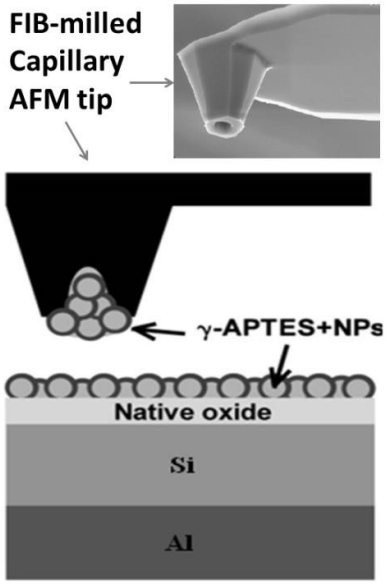

Figure 1. γ-APTES+NPs membrane coated by using the FIB-milled capillary AFM tip. The inset shown is the SEM image of the FIB-milled capillary AFM tip.

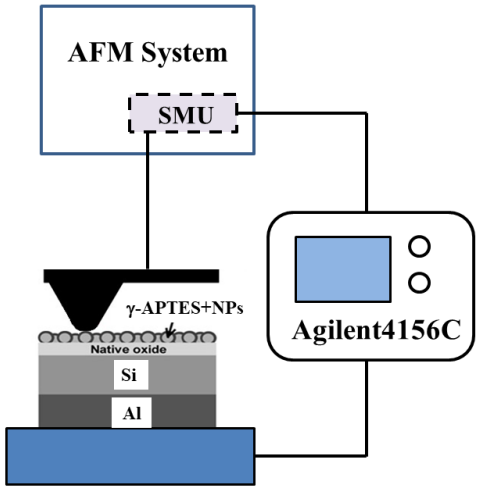

Figure 2. Measurement structure of the γ-APTES+NPs film using the conductive AFM tip as the top electrode.

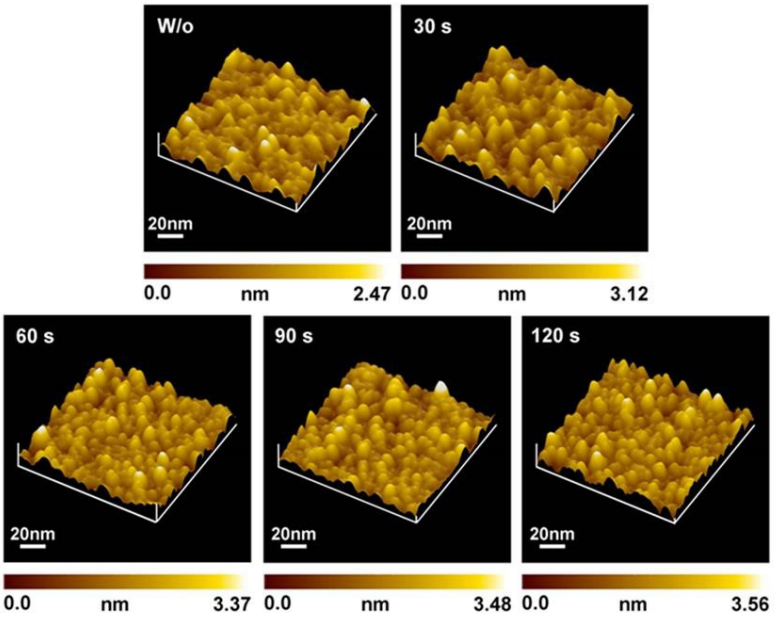

Figure 3. AFM surface morphology images of the γ-APTES+NPs membrane (with a γ-APTES solution/NPs mixed ratio of 100:1) after being subjected to UV light illumination with exposure time varying from 0 to 120 s.

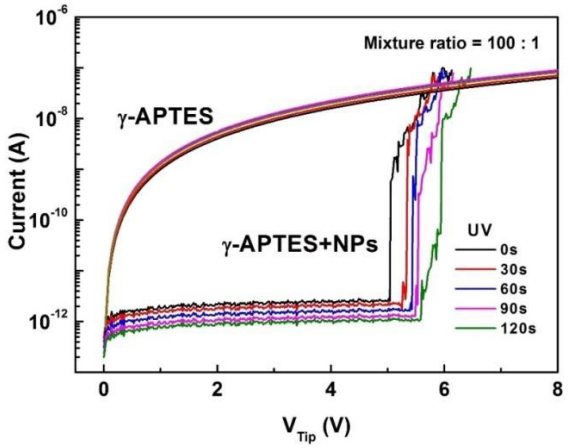

Figure 4. Nanoscale bulk leakage currents of γ-APTES and γ-APTES+NPs (with a γ-APTES solution/NPs mixed ratio of 100:1) membranes after being subjected to UV light illumination with various exposure times as a function of AFM tip voltage measured by placing a conductive PtIr AFM tip on the membrane surface.

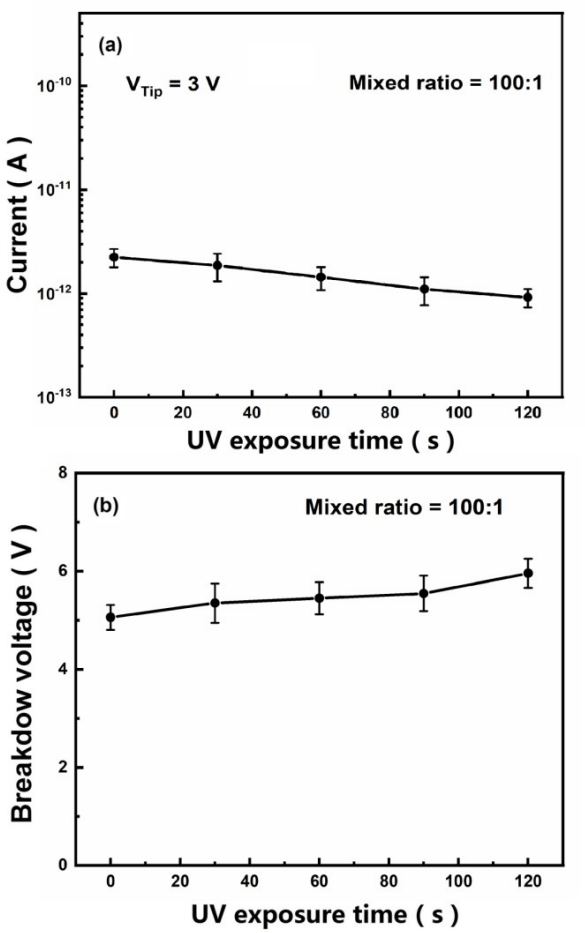

Figure 5. (a) Nanoscale bulk leakage currents at an AFM tip voltage of 3 V, and (b) the breakdown voltage of the γ-APTES+NPs membrane (with a fixed γ-APTES solution/NPs mixed ratio of 100:1) as function of UV light exposure time.

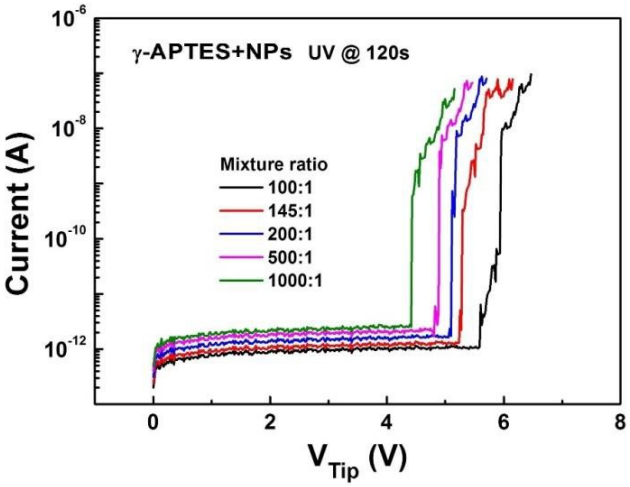

Figure 6. Nanoscale bulk leakage currents of the γ-APTES+NPs membrane with various γ-APTES solution/NPs mixed ratios after being exposed to 120 s UV light illumination as a function of AFM tip voltage measured by placing a conductive PtIr AFM tip on the membrane surface.

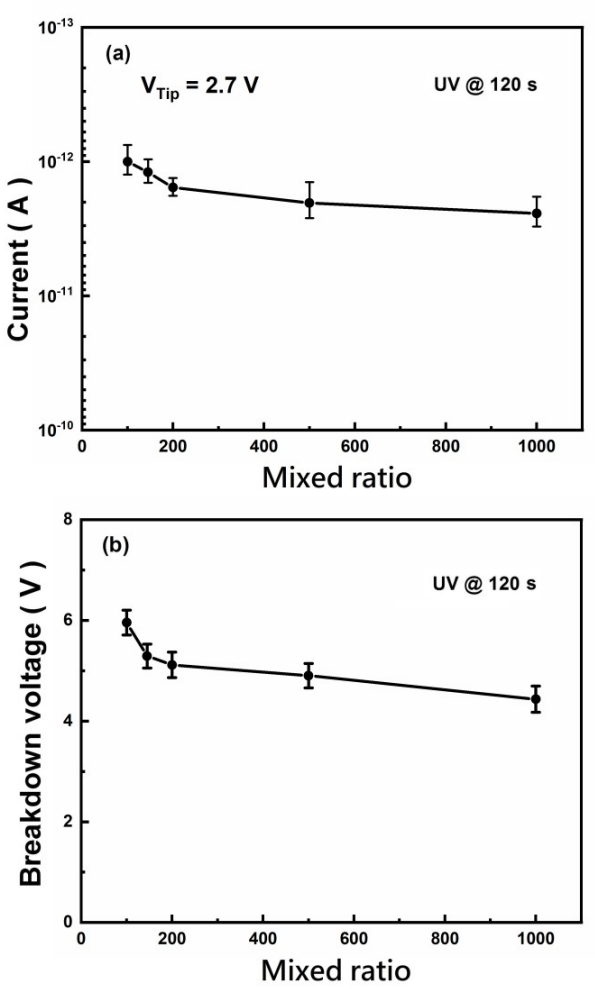

Figure 7. (a) Nanoscale bulk leakage currents at an AFM tip voltage of 2.7 V, and (b) breakdown voltage of the γ-APTES+NPs membrane after being exposed to 120 s UV light illumination as a function of various γ-APTES solution/NPs mixed ratios.

4. Discussion

According to our previous investigation, the ethoxy groups in γ-APTES can react with Si-OH and form Si-O-Si bonds on the oxide surface after a 120℃, 5 min curing process [6]. Therefore, the Si-OH bonds on the NPs surface, as well as the additional induced Si-OH bonds caused by UV exposure, will increase the reaction probability with the ethoxy group of the γ-APTES, forming more Si-O-Si bonds and improving membrane quality [19, 20]. This explains why that the nanoscale bulk leakage current decreases, while the average breakdown voltage increases, with the increase of the UV light exposure time, as given in Figs 5(a) and 5(b). On the other hand, increasing the percentage of silica NPs in γ-APTES solution (i.e., decreasing the γ-APTES solution/NPs mixed ratio) and allowing a longer UV exposure time will increase the number of Si-O-Si bonds in the membrane, thus making the binding network in the membrane denser and producing a higher quality of the membrane. Hence, the nanoscale bulk leakage current increases, while the average breakdown voltage decreases, with increasing γ-APTES solution/NPs mixed ratio as shown in Figs. 7(a) and 7(b). It is also found that, for the γ-APTES+NPs membrane, the mixed weight ratio of 100:1 is the most suitable ratio, attributable to the poor dispersion of nanoparticle clusters due to cohesive force among NPs in the membrane with mixed ratios smaller than 100:1.

5. Conclusions

This work evaluated the nanoscale bulk leakage current of γ-APTES-based films prepared with different NPs mixed ratios, as well as various UV light exposure times, deposited by a FIB-milled capillary AFM tip. The nanoscale I-V characteristics of the γ-APTES, as well as the γ-APTES+NPs films, were measured by using a conductive AFM connected with the semiconductor parameter analyzer Agilent 4156C. It is found that the I-V characteristic of the γ-APTES membrane with the incorporation of PDMS-treated silicate NPs can act as a dielectric-like material, in which there is a sudden current increase at a certain voltage, which is similar to the dielectric breakdown. Our experimental results demonstrate that not only can the bulk structure sustain a high electric field, but the bulk leakage current can also be greatly improved when the γ-APTES membrane is incorporated with silicate NPs. It is also determined that the breakdown voltage, as well as the bulk leakage current, can be improved by increasing the mixed weight ratio of γ-APTES solution/NPs, and the film quality is able to be further improved with the assistance of UV light exposure treatment.

Author Contributions: conceptualization, J.-J. Lin and Y.-L. Wu; methodology, J.-J. Lin and J.-J. Jhuang.; validation, J.-J. Lin and Y.-L. Wu; formal analysis, S.-Y. Liao and J.-J. Jhuang; investigation, S.-Y. Liao and J.-J. Jhuang; resources, J.-J. Lin, Y.-L. Wu, and C.T.-S. Ching; data curation, S.-Y. Liao, J.-J. Jhuang, and J.-J. Lin; writing—original draft preparation, S.-Y. Liao and J.-J. Lin; writing—review and editing, Y-L.Wu; visualization, S.-Y. Liao and J.-J. Lin; supervision, J.-J. Lin, Y.-L. Wu, and C.T.-S. Ching.

Funding: This research did not receive external funding.

Acknowledgments: The authors would like to express their sincere appreciation for financial support from the Ministry of Science and Technology, Taiwan, R.O.C. under contract no. MOST 103-2221-E-260-032 and MOST 107-2221-E-260-013.

Conflicts of Interest: The authors declare no conflict of interest.

References

1. Chen, Y.; Wang, X.; Erramilli, S.; Mohanty, P.; Kalinowski, A. Silicon-based nanoelectronic field-effect pH sensor with local gate control. *Appl. Phys. Lett.,* **2006**, *89*, pp. 223512-1–223512-3.
2. Hsu, P.Y.; Lin, J.J.; Wu, Y.L.; Hung, W.C.; Cullis, A.G. Ultra-sensitive polysilicon wire glucose sensor using a 3-aminopropyltriethoxysilane and polydimethylsiloxane-treated hydrophobic fumed silica nanoparticle mixture as the sensing membrane. *Sens. Actuators B* **2009**, *142*, pp. 273-279.
3. Wu, Y.L.; Hsu, P.Y.; Lin, J.J. Polysilicon wire glucose sensor highly immune to Interference. *Biosens. Bioelectron.* **2011**, *26*, pp. 2281– 2286.
4. Lin, J.J.; Hsu, P.Y.; Wu, Y.L.; Jhuang, J.J. Characteristics of polysilicon wire glucose sensors with a surface modified by silica nanoparticles/γ-APTES nanocomposite. *Sensors* **2011**, *11*, pp. 2796–808.
5. Wu, Y.L.; Hsu, P.Y.; Hsu, C.P.; Liu, W.C. Polysilicon wire for the detection of label free DNA. *J. Electrochem. Soc.* **2010**, *157*, pp. J191–195.
6. Wu, Y.L.; Lin, J.J.; Hsu, P.Y.; Hsu, C.P. Highly sensitive polysilicon wire sensor for DNA detection using silica nanoparticles/c-APTES nanocomposite for surface modification. *Sens. Actuator B.* **2011**, *155,* pp. 709–15.
7. Hahm, J.; Lieber, C.M. Direct ultrasensitive electrical detection of DNA and DNA sequence variations using nanowire nanosensors. *Nano Lett.* **2004**, *4*, pp. 451-54.
8. Hsu, C.P.; Hsu, P.Y.; Wu, Y.L.; Lee, E.; Chen,P.H.; Lin, J.J. Evolvement of cell-substrate interaction over time for cells cultivated on a 3-aminopropyltriethoxysilane (γ-APTES) modified silicon dioxide (SiO_2) surface. *Appl. Surf. Sci.* **2012**, *258*, pp. 8641–8648.
9. Wu, Y.L.; Hsu, P.Y.; Hsu, C.P.; Lin, J.J. Detecting the effect of targeted anti-cancer medicines on single cancer cells using a poly-silicon wire ion sensor integrated with a confined sensitive window. *Biomed. Microdevices.* **2012**, *14*, pp. 839–848.
10. Li, X.G.; Feng, H.; Huang, M.R.; Gu, G.L.; Moloney, M.G. Ultrasensitive Pb(II) potentiometric sensor based on copolyaniline nanoparticles in a plasticizer-free membrane with a long lifetime, *Anal. Chem.* **2012**, *84*, pp. 134–140.
11. Weber, M.; Kim, J.H.; Lee, J.H.; Kim, J.Y.; Iatsunskyi, I.; Coy, E.; Drobek, M.; Julbe, A.; Bechelany,M.; Kim, S.S. High-performance nanowire hydrogen sensors by exploiting the synergistic effect of Pd nanoparticles and metal-organic framework membranes. *ACS Appl. Mater. Interfaces* **2018**, *10*, pp. 34765–34773.
12. Ayesha, A.I.; Abu-Hanib, A.F.S.; Mahmoudc, S.T.; Haikd, Y. Selective H_2S sensor based on CuO nanoparticles embedded in organic membranes. *Sens. Actuator B.* **2016**, *231*, pp. 593-600.
13. Feng, Y.; Yang, T.; Zhang, W.; Jiang, C.; Jiao, K. Enhanced sensitivity for deoxyribonucleic acid electrochemical impedance sensor: gold nanoparticle/ polyaniline nanotube membranes. *Anal. Chim. Acta* **2008**, *616*, pp. 144-151.

14. Li, Y.; Zhang, P.; Ouyang, Z.; Zhang, M.; Lin, Z.; Li, J.; Su, Z.; Wei, G. Nanoscale graphene doped with highly dispersed silver nanoparticles: quick synthesis, facile fabrication of 3D membrane-modified electrode, and super performance for electrochemical sensing. *Adv. Funct. Mater.* **2016**, *26*, pp. 2122-2134.
15. Hong, J.; Lee,S.; Seo, J.; Pyo, S.; Kim, J.; Lee, T. A highly sensitive hydrogen sensor with gas selectivity using a PMMA membrane-coated Pd nanoparticle/ single-layer graphene hybrid. *ACS Appl. Mater. Interfaces* **2015**, *7*, pp. 3554−3561.
16. Kim, J.; Seidler, P.; Wan,L.S.; Fill, C. Formation, structure, and reactivity of aminoterminated organic films on silicon substrates. *J. Colloid. Interface Sci.* **2009**, *329*, pp. 114–119.
17. Lin, J.J.; Lin, S.H.; Wu, Y.L. Resistive switching in a metal-insulator-metal device with γ-APTES as the insulator layer. *Solid-State Electron.* **2017**, *136,* pp. 86–91.
18. Hsu, P.Y.; Lin, J.J.; Lai, B.W.; Wu, Y.L.; Yang, C.F. S.S. Lin, FTIR characterizations of the gamma-ray-irradiated silica nanoparticles/γ-APTES nanocomposite with UV annealing, in: J. Juang, Y.C. Huang (Eds.), Intelligent Technologies and Engineering Systems, E-Publishing Inc., New York, 2013, pp. 893-899.
19. Tian, R.; Seitz, O.; Li, M.; Hu, W.; Chabal, Y.J. J. Gao, Infrared characterization of interfacial Si-O bond formation on silanized flat SiO_2/Si surfaces. *Langmuir* **2010**, *26*, pp. 4563–4566.
20. Pena-Alonso, R.; Rubio, F.; Rubio, J.; Oteo, J.L. Study of the hydrolysis and condensation of γ-Aminopropyltriethoxysilane by FT-IR spectroscopy. *J. Mater. Sci.* **2007**, *42*, pp.595–603.
21. Wu, Y.L.; Lin, S.T.; Lee, C.P. Time-to-breakdown Weibull distribution of th in gate oxide subjected to nanoscaled constant voltage stress and constant current stress. *IEEE Trans. Device. Mater. Reliab.* **2008**, *8*, pp. 352 – 357.
22. Verweij, J.F.; Klootwijk, J.H. Dielectric breakdown I: A review of oxide breakdown. *Microelectronics J.* **1996**, *27*, pp. 611-622.